Electrochemistry at the Nanoscale: The Force Dimension

by Jennifer Black, Evgheni Strelcov, Nina Balke, and Sergei V. Kalinin

Progress in energy storage and conversion technologies necessitates understanding fundamental mechanisms of electrochemical processes, including intercalation, phase transformations, and surface electrochemical reactions, from atomic to mesoscopic levels. These processes are sensitively affected by the intricacies of electronic and ionic transport, as well as strain fields and mechanical processes. The key to successful understanding of these mechanisms lies in structural and functional imaging — namely obtaining spatially resolved information on the structure, properties, and all aspects of electrochemical functionality in 3D space and in time. Once available, this information can be used to establish local deterministic mechanisms and can further be used in predictive modeling, subsequently enabling knowledge-driven optimization of materials properties and structures, and providing an experimental counterpart to large-scale theoretical investigations as embodied in the Materials Genome program.

The structural imaging of electrochemical systems can be achieved using classical techniques including (scanning) transmission electron microscopy, X-ray tomography, and atom probe tomography. The challenge is whether locally measured structural information and its evolution with time (*e.g.*, in *in situ* electrochemical experiments) is correlated with macroscopically-averaged functional behaviors to develop a full 3D picture of electrochemical process dynamics, from which one can extract local constitutive relations that can be further used in formulating high-veracity theoretical models. Notably, the number of degrees of freedom in realistic macroscopic systems, as determined by number of grains, defects, and ultimately atoms, is extremely large and even if available experimentally, integration into the theoretical models is a challenge. Hence, the development of simplified model systems amenable to structural and macroscopic functional studies is of great interest. This brings forth the question of what is the minimally complex system that will still contain relevant functionality of, *e.g.*, a battery device, but will remain amenable to local studies, from which information can be extracted and deployed to stochastic models.

Complementary to this approach is functional electrochemical imaging. The key questions herein are whether charge-discharge, electronic and ionic transport, and other aspects of electrochemical behavior can be studied at the level of single particle or relevant structural element, whether the relevant local mechanisms can be established, and whether this knowledge can be extrapolated to the macroscopic assembly scale. Functional imaging necessitates the development of probes for individual aspects of functionality, including local ionic concentrations, electrochemical potentials, strains, reaction rates, and integrating them in single- and multimodal detection methods. This, in turn, requires the capability to manipulate electrochemical degrees of freedom locally, *i.e.*, change local potentials, electrochemical potentials, and detect associated material responses.

In this article, we present several paradigms for probing local electrochemical functionalities using force-based scanning probe microscopy (SPM). Force based SPMs rely on the concept of a cantilevered tip interacting with a surface.[1] As applied to electrochemical problems, the tip can serve as a mobile electrode, confining the electric field to a small volume of material and inducing relevant electrochemical transformations. At the same time, the tip acts a force, displacement, or current sensor. In force detection mode, the AFM can detect the local work function above the surface, directly related to local electrochemical potentials.[2-5] In the displacement detection mode, the SPM can detect static (of order of ms – minutes) or dynamic (> kHz) bias-induced strains directly related to electrochemical polarization.

The majority of electroactive materials used in batteries, electrochemical capacitors, or fuel cells, have one feature in common in that the unit cell volume or the sample volume is directly connected to ionic concentration (Vegard law) in the lattice[6,7] or the ion concentration in electrode pores.[8] This intrinsic link between ionic and mechanical phenomena offers a pathway for probing ionic concentration and mobility through mechanical strain. SPM is able to measure height changes down to ~1 pm in the dynamic detection modes (imaging at cantilever resonances), which facilitates obtaining information from regions on the order of the tip size, *i.e.*, spatially resolved information about ionic transport in the tens of nm range, well beyond the range of classical current based detection techniques. This approach is adopted in Electrochemical Strain Microscopy (ESM).[9]

Here, we differentiate between static and dynamic ESM. In static ESM (dilatometry), the tip acts as a passive strain sensor that allows performing ESM measurements in a fully functional electrochemical device. This method was applied for electrochemical capacitors.[10] In nanoporous carbon electrodes, ions enter the pores during charging to form the electrical double layer (EDL) and balance charge on the electrode surface. The flux of ions into the pores and formation of the EDL in such confined spaces is associated with internal stain and hence an increase in the electrode volume, which is easily detectable using AFM. Monitoring the volume changes *in situ* provides a non-current based method of tracking the ionic fluxes within nanoporous materials. Figure 1a shows the *in situ* electrochemical AFM cell, which has a planar design allowing easy access of the AFM tip to the working electrode without interference from the counter electrode. The capacitance of porous carbons with different surface area in $Emim^+$ Tf_2N^- (1-ethyl-3methyl-imidazolium bis(trifluoromethanesulfonyl)imide) ionic liquid electrolyte, and the corresponding height change (plotted as stress to account for the different Young's modulus) are shown in Fig. 1b and c, respectively. The stress profile in each case is parabolic with respect to applied charge. The strain behavior is strongly linked to the sample preparation and porosity as reported in [10].

This approach further allows the kinetics of the ion insertion process to be explored. Figure 1d shows a spectrogram of the relative height change of the as prepared mesoporous carbon (MC) carbon film over three cyclic voltammogram cycles at various sweep rates between 0.5 and 500 mV s^{-1}. At fast sweep rates there is a broad strain response, and as the sweep rate is reduced, a maximum in the strain is observed at the maximum anodic and cathodic potentials. Figures 1e and f show the phase shift between the stress and applied potential for the anodic and cathodic peaks, respectively. At fast sweep rates, there is a large phase shift which decays with decreasing sweep rate until equilibrium is attained at a phase shift of 0 degrees. In this regime the ions have sufficient time to follow the changes in applied potential. The activated carbon sample with the smallest pores shows the slowest kinetics for both the cathodic and anodic ion insertion processes, and the cathodic process exhibits faster kinetics than the anodic process in all carbons examined. Using this strain based technique the anodic and cathodic processes could easily be separated, and the effect of pore size on the kinetics of the ion insertion/adsorption processes could be ascertained.

Compared to electrochemical capacitors, the ionic mobility in Li-ion batteries is drastically reduced due to charge storage based on intercalation or phase changes instead of ion insertion into electrode pores. Here, the approach of static ESM becomes insufficient and dynamic ESM is applied to characterize ionic processes. In dynamic ESM, the AFM tip is biased with an AC voltage to induce local changes in ion concentration and the resulting dynamic

(continued on next page)

electrode expansion is measured. In this case, multiple effects can contribute to measured response, including Vegard-type volume changes, the formation of electrochemical dipoles, injection of charges from the tip, and electrostatic interactions between the SPM tip and surface charges.[11-13]

Several key experiments can be performed to identify different signal origins in dynamic ESM. One of them is the measurement of surface response as a function of temperature. This has been done for RF-sputtered $LiCoO_2$ films on Au/Al_2O_3 substrates.[14] The surface displacement as a result of the applied AC voltage increases with increasing temperature as shown in Fig. 2a for three different temperatures. It can be seen that the local displacement is quite heterogeneous across the sample. Since the measurement was performed in the exact same location, it is possible to construct Arrhenius plots for each pixel of the map and extract the activation energy for each location. The resulting map and the corresponding topography are shown in Fig. 2b and c. The averaged activation energy is about 0.26 eV, which fits well with numbers from theory and other macroscopic characterization techniques for $LiCoO_2$, typically around 0.3 eV. This is an indicator that the measured surface displacement is indeed connected to the motion of Li-ions. Here, ESM allows the activation energy dispersion to be examined and correlated with the microsctructure with a lateral resolution of 20-30 nm, which is not possible with other characterization techniques.

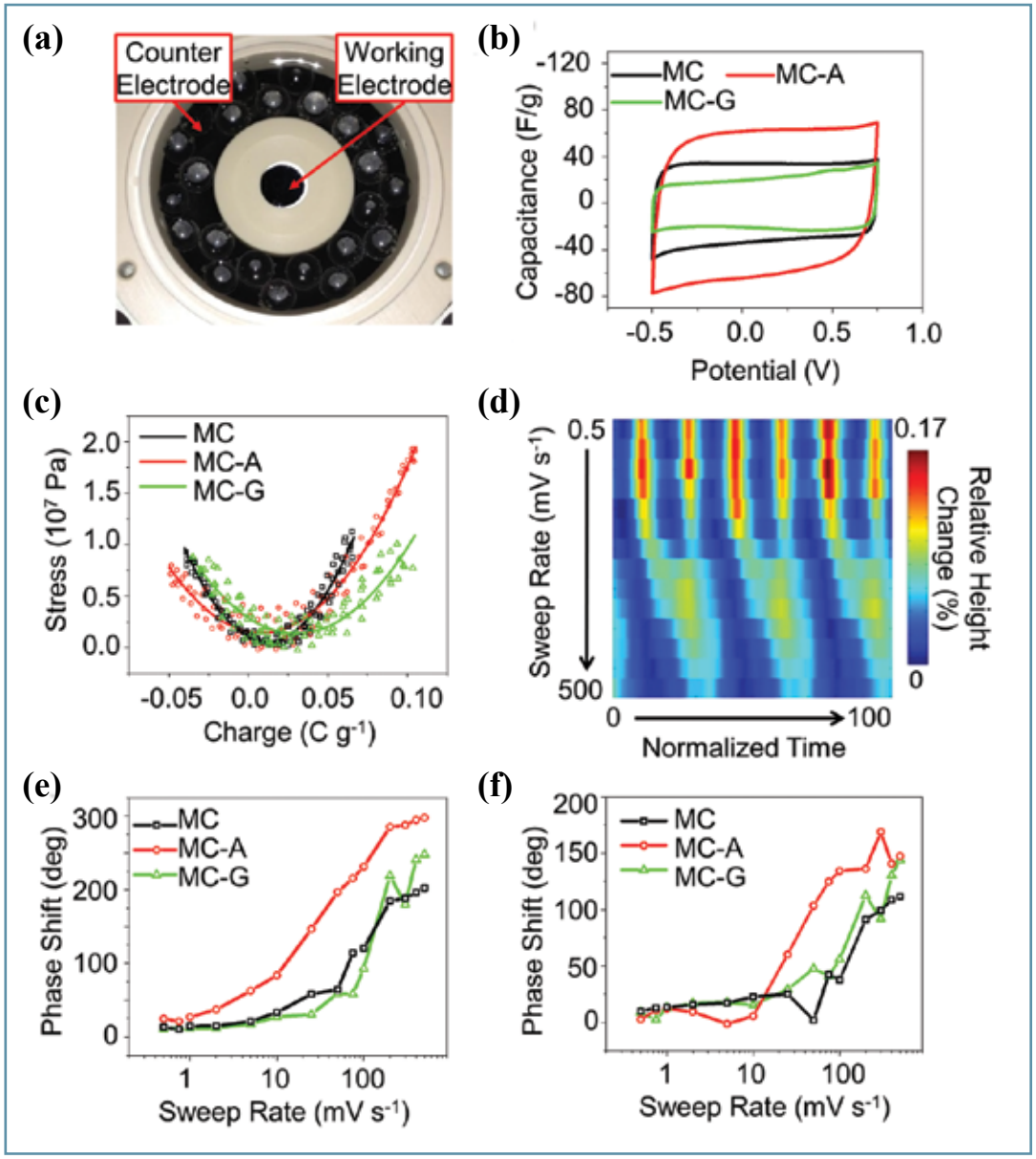

Fig. 1. *(a) Photograph of the electrochemical AFM cell (top view). (b) Capacitance and (c) stress as a function of applied charge (as well as polynomial used to fit the data) of MC, MC-A, and MC-G carbon membranes at a sweep rate of 0.5 mVs^{-1} in EMI$^+$TFSI$^-$ electrolyte. (d) Spectrogram of relative height change of MC carbon membrane in EMI$^+$TFSI$^-$ electrolyte during three CV cycles at sweep rates between 0.5 and 500 mV s^{-1}. Phase shift between applied potential strain response for anodic (e) and cathodic (f) peaks for MC, MC-A, and MC-G carbon membranes as a function of sweep rate. Figure adapted from ref. [10].*

The ESM technique was demonstrated experimentally for a variety of electrochemically active model systems, most notably $LiCoO_2$ cathodes[15] and Si anodes.[16] In $LiCoO_2$, it was possible to identify grains and grain boundaries with enhanced Li-ion kinetics. Subsequently, using a model amorphous Si anode (a-Si) surface, the local Li-ion flow and the microstructure of a $LiCoO_2$/LiPON/a-Si all-solid thin film battery was investigated. It was found that the microstructure, which showed grain-like features separated by boundaries, is strongly correlated with Li-ion transport through the amorphous Si anode, suggesting the existence of Li-ion conduction channels[16] and opening the pathway towards exploring the evolution of Li-ion dynamics as a function of state of charge of batteries during operation. A similar approach was applied to oxygen conductors including YSZ[17] and LSCO.[18-20]

These first demonstrations of ESM have stimulated ongoing efforts focusing on the description of corresponding image formation mechanisms at the *mesoscopic* level, with the ultimate goal of rendering ESM *quantitative*. The phase-field modeling of ESM contrast as a function of local crystallographic orientation is reported in [21]. The ESM technique has further been extended to a range of spectroscopic techniques that allow real-space mapping of the diffusion and electrochemical phenomena in solids. The use of low-frequency (~1 Hz) voltage sweeps allows local ion dynamics to be probed, because these time scales are directly comparable with diffusion times of ions on the 1-10 nm length scale.[16] Detailed insights into the relaxation phenomena through time-resolved spectroscopic measurements have been obtained and image formation mechanisms have been explored using the synergy of

analytical theory and numerical modeling.[22] Finally, ESM has been extended to probe irreversible electrochemical processes, such as nucleation of Li-nanoparticles on solid electrolytes.[23, 24]

While ESM addresses electrochemical phenomena at tip-surface junctions, SPM can be further adapted to probe lateral ionic transport across the surface. In this case, ionic motion is induced using a system of patterned electrodes, whereas the SPM tip is used as a non-invasive probe of local potentials. Kelvin Probe Force Microscopy (KPFM)[2-5] maps the contact potential difference between the tip and sample. Lateral charge transport (both electronic and ionic) in the frequency domain can be measured with the Scanning Impedance Microscopy technique[25] and its non-linear analogs.[26] Finally, time-resolved KPFM[27] has been specifically developed for probing ionic dynamics in lateral devices in real time.

A schematic of the time-resolved (tr)-KPFM is shown in Fig. 3a. The sample is polarized by a step-waveform DC bias applied between two lateral electrodes. A conductive SPM cantilever oscillates at a pre-defined distance above the surface, being mechanically driven at a frequency close to the free resonance (ω_0). A constant DC offset and an ac excitation bias at frequency ω away from ω_0 is applied to the tip. Local electrostatic interactions between the tip and surface are detected by the lock-in amplifier, and can further be calibrated to yield the surface potential. Figures 3b-e show temporal evolution of potential profiles in bias *on* and *off* states as measured on a Ca-substituted $BiFeO_3$ film.[27] This material possesses an ionically-mediated metal-insulator transition, during which a bias-driven redistribution of oxygen vacancies leads to a three orders of magnitude increase in electronic conductivity. A pristine Ca-BFO film (in its insulating state) shows accumulation/dissipation of negative ions by the biased electrode in the *on/off* states, respectively (negative potential pits in Fig. 3c-d). The measured activation energies of these processes are close to that of the proton transport in bulk water (0.13 vs. 0.12 eV), which indicates that the accumulated ions can be ascribed to the surface hydroxyl groups. The measured diffusivity is $2 \cdot 10^{-9}$ m^2/s, as compared to $\sim 10^{-8}$ m^2/s for proton in water.

At the same time, devices pre-activated by high bias reveal formation of a virtual electrode — a region where the film has switched into the metallic state (Fig. 3e). The rest of the film accumulates a positive charge during the bias-*on* process and slowly dissipates the charge when the electrodes are grounded. The nature of this charge remains elusive, as it can originate from either the oxygen vacancies or from the electronic holes. Similar experiments performed on $LiNbO_3$ ferroelectric surfaces[28] showed strong charge injection from the biased electrode, presumably due to electrochemical water splitting on the surface with subsequent electromigration of protons onto the film.

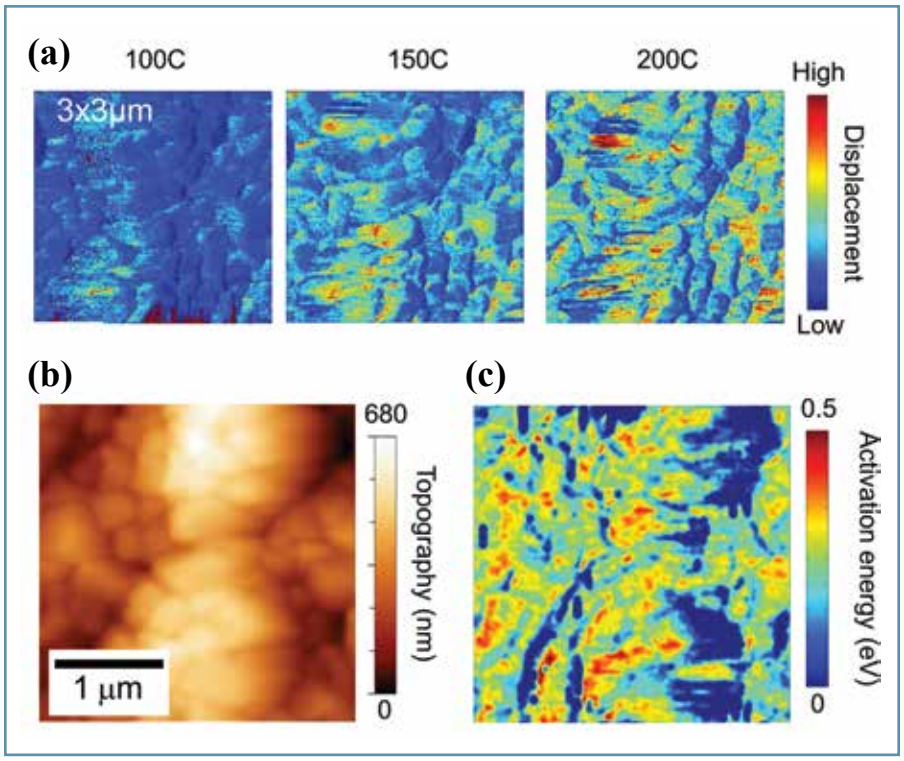

Fig. 2. *Dynamic ESM as function of temperature (a) in the same region of the sample (b). (c) The extracted spatial map of activation energy. Figure adapted from ref. [14].*

Finally, SPM sensitivity to weak forces enables extending this approach for probing electrochemistry on the molecular level, as exemplified by the structure of double layers. In force-volume measurements, the tip approaches a charged surface in the liquid and the deflection of the tip is recorded as a function of distance to the sample surface. In the presence of layered structures in the liquid, the tip feels oscillating forces when approaching the sample. This behavior is especially pronounced for ionic liquids,[29-35] which are promising materials for electrolytes in energy storage systems. At the electrode interface, ionic liquids form an alternating structure of anion/cation layers, and AFM force spectroscopy is capable of probing this layered structure. This technique was used to investigate the structure of ionic liquid-solid interfaces,[29-32] and recently was extended to probe the electrical double layer at a carbon interface at different applied bias.[36] Sub-nanometer ion layer spacings were observed experimentally and compared to molecular dynamics (MD) simulations, with excellent agreement between the predicted and experimentally observed ion layer positions. Figure 4 shows the experimental force data (> 50% probability) for the unbiased carbon compared with the MD ion density profiles for the anion (Fig. 4a) and cation (Fig. 4b). The MD ion profiles show a double peak in the near-surface region due to different orientations of ions (parallel and perpendicular) at the electrode surface. The experimental data also shows two closely spaced ion layers in this region illustrating that this technique is capable of differentiating between two different ion orientations at the electrode surface. Further from the surface, the force data matches closely with the positions of the anion layers predicted by MD. The structure of the ionic liquid within the electrical double layer is altered under applied bias compared to the unbiased case through the addition of Coulombic forces between the ions and electrode, and this reconfiguration of the ionic structure can be observed using force spectroscopy. Figures 4e and f show the ion density profiles for the cation (Fig. 4e) and anion (Fig. 4f), calculated by MD, as a function of potential and distance from the electrode surface. At 1 V bias the first ion layer consists primarily of anions, whereas it is populated by cations at -1 V. In both cases, the ions preferentially orient parallel to the electrode surface. Through the integration of experiment and theory, a comprehensive picture of the structure of the electrical double layer at charged and uncharged carbon in ionic liquid electrolytes is achieved, improving our understanding of charge storage on a molecular level. This technique can be further extended to perform force-volume mapping to investigate the spatial variation and examine the effects of features such as surface defects on the ionic liquid structure at the interface.

This article summarizes some of the scanning probe microscopy based strategies for interrogating local electrochemical and ion transport processes based on local probing

(continued on next page)

and device-like configurations. While SPM can be envisioned as a nanoscale electrode, transition to the nanoscale all but excludes classical electrochemical strategies based on detection of faradaic and capacitive currents. However, SPM can access the broad panoply of parameters indirectly related to the electrochemical state of the system, including local potentials, strain response, and conductive currents. Extending beyond the force-based techniques discussed here, hysteresis in conductive currents can be used to map electrochemical processes at the sub-10 nanometer and, potentially, atomic levels.[37, 38]

The challenge in these techniques is twofold. The first challenge is the proper calibration of the system, *i.e.*, determination of the absolute response of the material, *e.g.*, surface deformation (nm), dynamic electromechanical response (nm/V), current hysteresis, and so on. The second challenge is analysis of the corresponding phenomena, *i.e.*, relating measured responses to parameters of interest, including Vegard coefficients and electrostriction constants, diffusion coefficients and mobilities, ionic concentrations, and bias dependent reaction rates. Related to this challenge is the separation of multiple responses, *e.g.*, piezochemical strains and electrostatic forces. While complex in general, the huge promise of this line of research is hard to exaggerate — basically, it provides the pathway for quantitative electrochemical measurements below the 10 nm level at the level of veracity of classical electrochemical techniques such as impedance spectroscopy.

More complex is the issue of undetermined surface states in electrochemical systems, which can be significantly different from the bulk due to surface reconstructions, contamination effects, etc. This problem is not unlike that in the classical surface science of semiconductors and metals. However, these systems allow for probing in the ultrahigh vacuum environment, where the surface is stabilized kinetically. For electrochemical systems, this approach is inapplicable, since our interest is functionality related to ionic motion and reactions. Correspondingly, this will require imaging under *in situ* and *in operando* conditions, while maintaining the electrochemical potential of a volatile component. In many cases, this will require development of specialized SPM systems, including high pressure high temperature cells for solid oxide fuel cells (SOFCs) and polymer electrolyte membrane (PEM) fuel cells and electrochemical probes for imaging in liquid electrolytes.

Finally, SPM generally allows only mesoscopic information to be gathered. *In situ* combinations of SPM as a local method to induce local electrochemical reactions with high resolution structural or chemical probes is an emergent area of great interest. This includes *in situ* SPM — scanning transmission electron microscopy to image atomic structures and chemical states by electron energy loss spectroscopy (EELS) imaging[39] (see manuscript by Borisevich, *et al.*, in this issue), SPM-focused X-ray to map local crystal structure changes, and SPM-near field optical spectroscopies to gain local chemical information. All of these present exciting possibilities for the future.

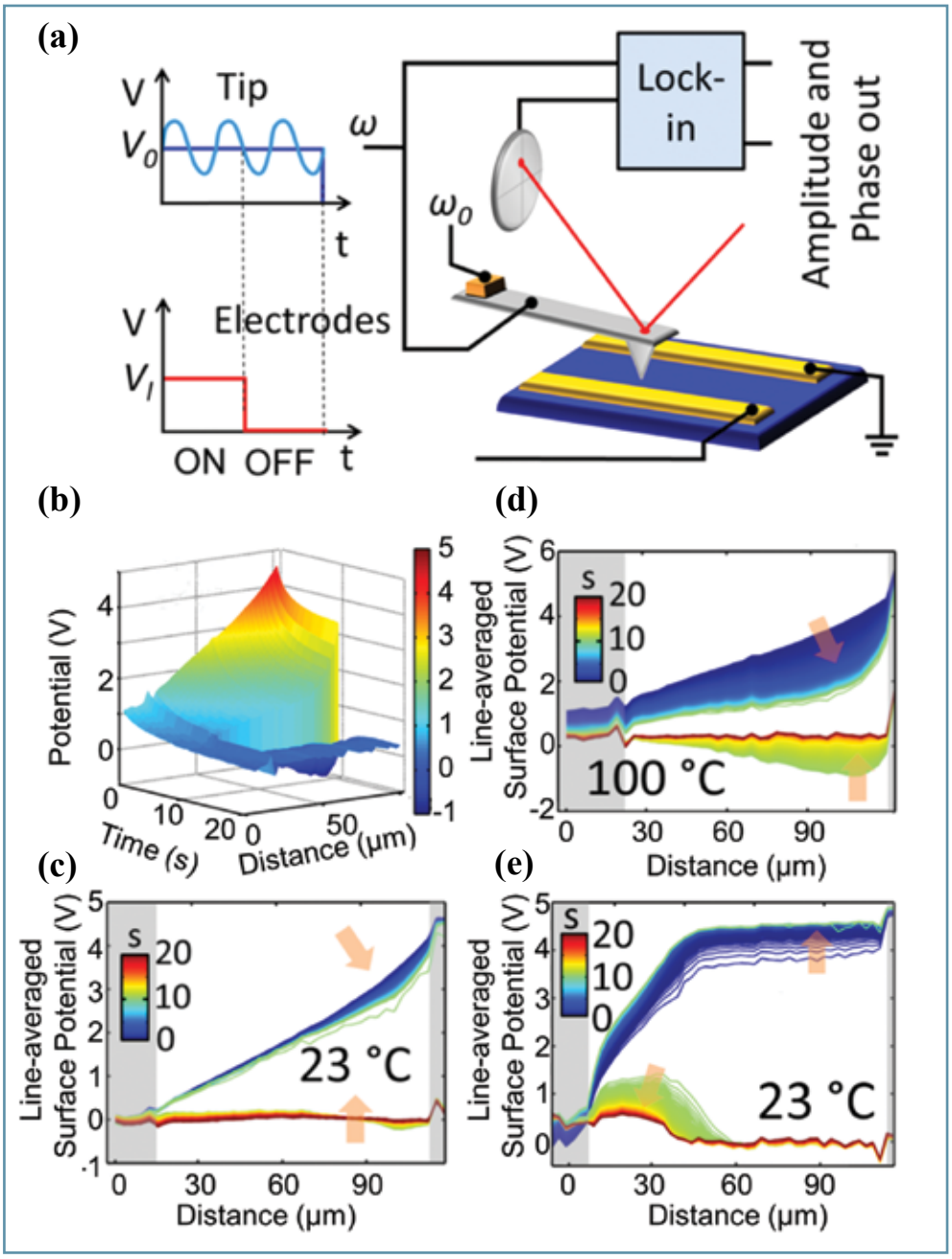

Fig. 3. *Surface ionic dynamics in lateral devices: (a) Schematic of the tr-KPFM technique; (b) 3D plot of surface potential in Ca-BFO as a function of time and distance; note how potential drops at t = 10s, as the electrode bias is switched off; (c) – (e) temporal evolution of the surface potential profiles at different temperatures and polarizing biases; panels (c) and (d) show data for a pristine device, panel (e) for pre-activated film; arrows indicate direction of change over time; note formation of a virtual electrode in panel (e). Figure adapted from ref. [27].*

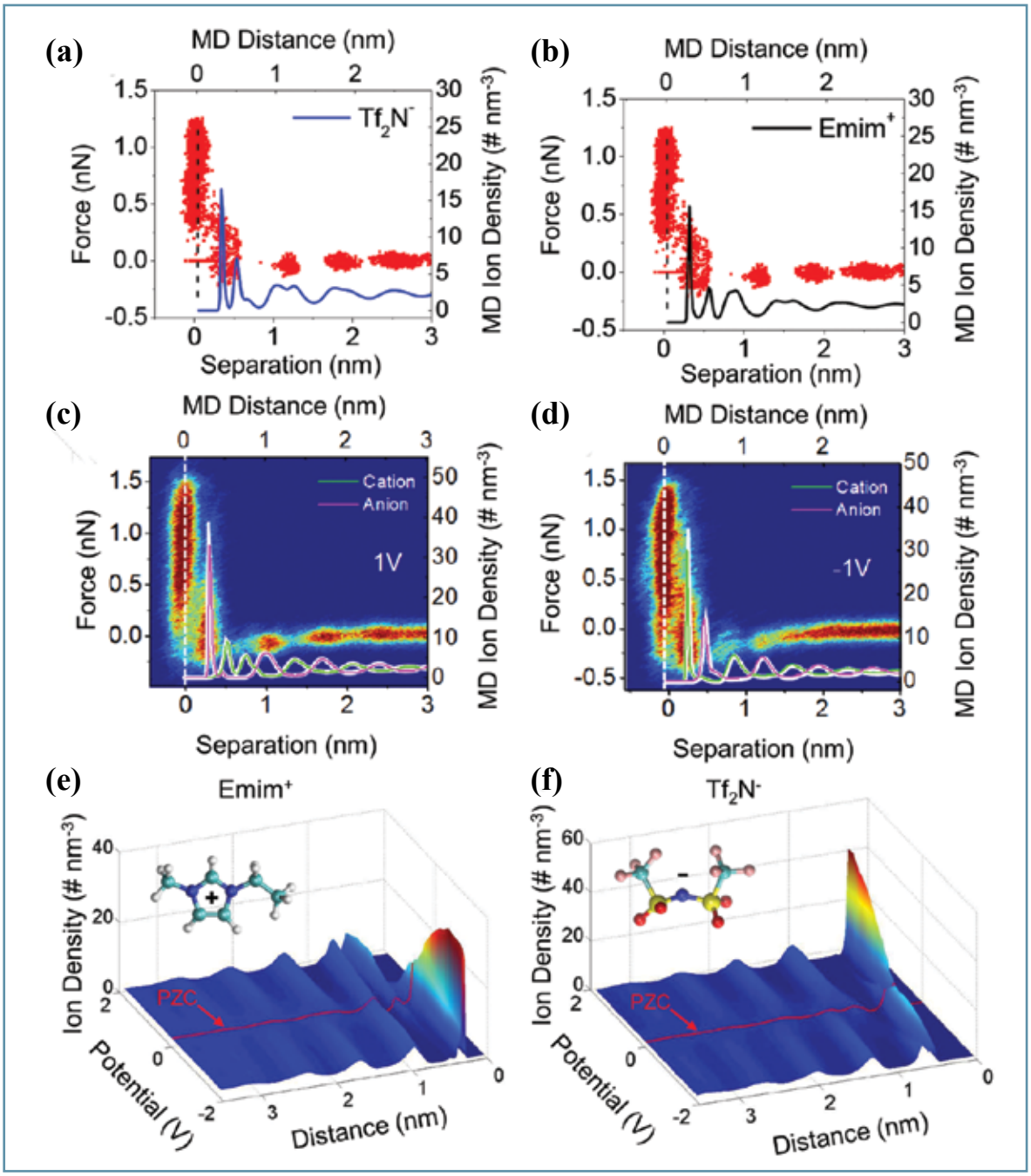

Fig. 4. *Comparison of the anion (a) and cation (b) MD density distribution and the experimental force data (> 50% probability) at the PZC. Comparison of experimental force separation curves under bias as 2-d histogram with MD simulations of cation and anion positions for positive (c) and negative potentials (d). The white line denotes the position of the electrode surface. Number density profiles of cations (e) and anions (f) near the electrode surface as a function of applied potential. The potential of zero charge (PZC) is indicated as a red line. Figure adapted from ref. [36].*

Acknowledgments

Static ESM and force volume experiments (JB) were supported by the Fluid Interface Reactions, Structures and Transport (FIRST), an Energy Frontier Research Center funded by the U.S. Department of Energy, Office of Science, Office of Basic Energy Sciences. Dynamic ESM experiments (NB) were supported by the U.S. Department of Energy, Basic Energy Sciences, Materials Sciences and Engineering Division through the Office of Science Early Career Research Program. tr-KPFM experiments (ES) and support for SVK were provided by the Center for Nanophase Materials Sciences, which is sponsored at Oak Ridge National Laboratory by the Scientific User Facilities Division, Office of Basic Energy Sciences, U.S. Department of Energy.

(continued on next page)

About the Authors

Jennifer Black received her BSc in Chemistry from Cape Breton University in 2006. She did her PhD at Dalhousie University under the supervision of Professor Heather Andreas focusing on the self-discharge mechanisms of electrochemical double-layer capacitors. From 2011-2012 she worked as a postdoctoral researcher at the Ohio State University in the group of Dr. Anne Co researching anode materials for lithium ion batteries and developing metallic foams for catalysis. She joined Oak Ridge National Laboratory as a postdoctoral researcher in 2012 where her current research focuses on the nanoscale characterization of energy storage materials using scanning probe microscopy. She may be reached at blackjm@ornl.gov.

Evgheni Strelcov has been a Postdoctoral Associate at the Oak Ridge National Laboratory since 2011. He received his PhD in Applied Physics in 2011 from Southern Illinois University and MS degree in Inorganic Chemistry in 2004 from Moldova State University, Moldova. He has published about 30 papers and been recognized with several distinguished awards, including Government Scholarship from Moldovian Prime Minister. His research interests include advanced scanning probe microscopy, bias-induced transformations in low dimensional materials, and gas sensorics. He may be reached at strelcove@ornl.gov.

Nina Balke is a research staff member in the Center for Nanophase Materials Sciences (CNMS) at Oak Ridge National Laboratory in Oak Ridge, TN. In 2006, she earned her PhD in Materials Sciences at the Technical University of Darmstadt in Germany working with ferroelectric ceramics. After being a Feodor-Lynen fellow at the University of California in Berkeley in the group of R. Ramesh she transitioned to CNMS in 2009 and is now working on nanoscale characterization of electromechanical effects in oxides focusing on energy storage materials. Her work was awarded the Department of Energy Early Career Research Award in 2011 and the American Ceramic Society's Robert L. Coble Award for Young Scholars in 2013. She may be reached at balken@ornl.gov.

Sergei V. Kalinin is a distinguished research staff member at the Center for Nanophase Materials Sciences (CNMS) at Oak Ridge National Laboratory and a Theme leader for Electronic and Ionic Functionality on the Nanoscale (at ORNL since 2002). He also holds an Adjunct Associate Professor position at Department of Materials Science and Engineering at the University of Tennessee-Knoxville, and Adjunct Faculty position at Pennsylvania State University. He received my PhD from the University of Pennsylvania in 2002, followed by the Wigner fellowship at ORNL (2002-2004). Sergei is a recipient of the Presidential Early Career Award for Scientists and Engineers (PECASE) in 2009, Burton medal of Microscopy Society of America in 2010, American Vacuum Society 2008 Peter Mark Memorial Award, 2010 and 2008 R&D100 Awards, 2003 Ross Coffin Award and 2009 Robert L. Coble Awards of American Ceramics Society, and a number of other distinctions. His research interests include coupling between electromechanical, electrical and transport phenomena on the nanoscale. Sergei has published over 300 peer-reviewed publications and edited 3 books. He has organized numerous symposia and workshops, including an International workshop series on Piezoresponse Force and Electrochemical Strain Microscopies held at 16 locations worldwide. He may be reached at sergei2@ornl.gov.

References

1. G. Binnig, C. F. Quate, and C. Gerber, *Phys. Rev. Lett.*, **56**, 930 (1986).
2. S. Sadewasser and T. Glatzel, *Kelvin Probe Force Microscopy: Measuring and Compensating Electrostatic Forces*, p. 331, Springer-Verlag, New York (2012).
3. W. Melitz, J. Shen, A. C. Kummel, and S. Lee, *Surf. Sci. Rep.*, **66**, 1 (2011).
4. A. Liscio, V. Palermo, and P. Samorì, *Accounts Chem. Res.*, **43**, 541 (2010).
5. H. Kim and D.-W. Kim, *Appl. Phys. A*, **102**, 949 (2011).
6. G. G. Amatucci, J. M. Tarascon, and L. C. Klein, *J. Electrochem. Soc.*, **143**, 1114 (1996).
7. X. Y. Chen, J. S. Yu, and S. B. Adler, *Chem. Mater.*, **17**, 4537 (2005).
8. M. M. Hantel, V. Presser, R. Kötz, and Y. Gogotsi, *Electrochem. Commun.*, **13**, 1221 (2011).
9. A. N. Morozovska, E. A. Eliseev, and S. V. Kalinin, *Appl. Phys. Lett.*, **96** (2010).
10. J. M. Black, G. Feng, P. F. Fulvio, P. C. Hillesheim, S. Dai, Y. Gogotsi, P. T. Cummings, S. V. Kalinin, and N. Balke, *Adv. Energy Mater.*, **4**, 1300683 (2014).
11. A. N. Morozovska, E. A. Eliseev, S. L. Bravina, F. Ciucci, G. S. Svechnikov, L. Q. Chen, and S. V. Kalinin, *J. Appl. Phys.*, **111** (2012).
12. A. N. Morozovska, E. A. Eliseev, and S. V. Kalinin, *J. Appl. Phys.*, **111** (2012).
13. A. N. Morozovska, E. A. Eliseev, A. K. Tagantsev, S. L. Bravina, L. Q. Chen, and S. V. Kalinin, *Phys. Rev. B*, **8**[illegible] (2011).
14. N. Balke, S. Kalnaus, N. J. Dudney C. Daniel, S. Jesse, and S. V. Kalinin *Nano Lett.*, **12**, 3399 (2012).
15. N. Balke, S. Jesse, A. N. Morozovska E. Eliseev, D. W. Chung, Y. Kim, L Adamczyk, R. E. Garcia, N. Dudney and S. V. Kalinin, *Nat. Nanotechnol.*, **5** 749 (2010).
16. N. Balke, S. Jesse, Y. Kim, L Adamczyk, A. Tselev, I. N. Ivanov N. J. Dudney, and S. V. Kalinin, *Nano Lett.*, **10**, 3420 (2010).
17. A. Kumar, F. Ciucci, A. N. Morozovska S. V. Kalinin, and S. Jesse, *Nat. Chem.* **3**, 707 (2011).
18. A. Kumar, S. Jesse, A. N. Morozovska E. Eliseev, A. Tebano, N. Yang, and S. V. Kalinin, *Nanotechnology*, **24** 145401 (2013).
19. D. N. Leonard, A. Kumar, S. Jesse, M. D. Biegalski, H. M. Christen, E. Mutoro, E. J. Crumlin, Y. Shao-Horn, S. V. Kalinin, and A. Y. Borisevich, *Adv. Energy Mater.*, **3**, 788 (2013).
20. S. Doria, N. Yang, A. Kumar, S. Jesse, A. Tebano, C. Aruta, E. Di Bartolomeo, T. M. Arruda, S. V. Kalinin, S. Licoccia, and G. Balestrino, *Appl. Phys. Lett.*, **103**, 171605 (2013).
21. D. W. Chung, N. Balke, S. V. Kalinin, and R. E. Garcia, *J. Electrochem. Soc.*, **158**, A1083 (2011).
22. S. Jesse, N. Balke, E. Eliseev, A. Tselev, N. J. Dudney, A. N. Morozovska, and S. V. Kalinin, *ACS Nano*, **5**, 9682 (2011).
23. T. M. Arruda, A. Kumar, S. V. Kalinin, and S. Jesse, *Nanotechnology*, **23**, 325402 (2012).
24. T. M. Arruda, A. Kumar, S. V. Kalinin, and S. Jesse, *Nano Lett.*, **11**, 4161 (2011).
25. S. V. Kalinin and D. A. Bonnell, *J. of Appl. Phys*, **91**, 832 (2002).
26. L. S. C. Pingree, D. B. Rodovsky, D. C. Coffey, G. P. Bartholomew, and D. S. Ginger, *J. Am. Chem. Soc.*, **129**, 15903 (2007).
27. E. Strelcov, S. Jesse, Y.-L. Huang, Y.-C. Teng, I. I. Kravchenko, Y.-H. Chu, and S. V. Kalinin, *ACS Nano*, **7**, 6806 (2013).

28. E. Strelcov, A. V. Ievlev, S. Jesse, I. I. Kravchenko, V. Y. Shur, and S. V. Kalinin, *Adv. Mater.*, **26**, 958 (2014).
29. R. Atkin, N. Borisenko, M. Drueschler, S. Z. El Abedin, F. Endres, R. Hayes, B. Huber, and B. Roling, *Phys. Chem. Chem. Phys.*, **13**, 6849 (2011).
30. R. Atkin, S. Z. El Abedin, R. Hayes, L. H. S. Gasparotto, N. Borisenko, and F. Endres, *J. Phys. Chem. C*, **113**, 13266 (2009).
31. F. Endres, N. Borisenko, S. Z. El Abedin, R. Hayes, and R. Atkin, *Faraday Discuss.*, **154**, 221 (2012).
32. R. Hayes, N. Borisenko, M. K. Tam, P. C. Howlett, F. Endres, and R. Atkin, *J. Phys. Chem. C*, **115**, 6855 (2011).
33. S. Perkin, *Phys. Chem. Chem. Phys.*, **14**, 5052 (2012).
34. S. Perkin, L. Crowhurst, H. Niedermeyer, T. Welton, A. M. Smith, and N. N. Gosvami, *Chem. Comm.*, **47**, 6572 (2011).
35. R. Atkin and G. G. Warr, *J. Phys. Chem. C*, **111**, 5162 (2007).
36. J. M. Black, D. Walters, A. Labuda, G. Feng, P. C. Hillesheim, S. Dai, P. T. Cummings, S. V. Kalinin, R. Proksch,
37. Y.-H. Hsieh, E. Strelcov, J.-M. Liou, C-Y. Shen, Y-C. Chen, S. V. Kalinin, and Y.-H. Chu, *ACS Nano*, **7**, 8627,(2013).
38. E. Strelcov, Y. Kim, S. Jesse, Y. Cao, I. Ivanov, I. Kravchenko, C.-H. Wang, Y-C. Teng, L.-Q. Chen, Y. H. Chu, and S. V. Kalinin, *Nano Lett.*, **13**, 3455 (2013).
39. H. Chang, S. V. Kalinin, S. Yang, P. Yu, S. Bhattacharya, P. P. Wu, N. Balke, S. Jesse, L. Q. Chen, R. Ramesh, S. J. Pennycook, and A. Y. Borisevich, *J. Appl. Phys.* 110, 052014 (2011).